Table I. P-C Bond Lengths (r_{P-C}), the P-C Overlap Populations (p_{P-C}), and the Total Energies (E_{tot}) of $P(CH_3)_nH_{3-n}$ and $P(CF_3)_nH_{3-n}$ Calculated by STO-3G and STO-3G* Basis Sets[a]

molecule	r_{P-C}, Å	p_{P-C}[d]	$-E_{tot}$, au
CH_3PH_2	1.8440	0.2883	377.2213
	1.8320	0.3302 (0.3278)	377.2734
CF_3PH_2	1.9056	0.2516	669.5971
	1.8835	0.2901 (0.2867)	669.6519
$(CH_3)_2PH$	1.8452	0.2854	415.8105
	1.8340	0.3293 (0.3272)	415.8660
$(CF_3)_2PH$	1.9135	0.2472	1000.5552
	1.8897	0.2873 (0.2830)	1000.6152
$P(CH_3)_3$[b]	1.8467	0.2817	454.4010
	1.8361	0.3278 (0.3257)	454.4595
$P(CF_3)_3$[c]	1.9216	0.2413	1331.5103
	1.8973	0.2832 (0.2785)	1331.5747

[a] For each molecule, the numbers obtained from the STO-3G and STO-3G* basis sets are respectively given in the first and the second rows. [b] The experimental P-C bond length is 1.846 Å. [c] The experimental P-C bond length is 1.904 Å. [d] The numbers in parentheses represent the P-C overlap population calculated by using the STO-3G* basis set on the molecular geometry determined from the STO-3G basis set.

and $P(CF_3)_nH_{3-n}$ (n = 1-3) by employing ab initio SCF MO calculations with STO-3G and STO-3G* basis sets.[7] In our calculations, all the geometrical parameters other than the P-C bond lengths were taken from the experimental values of $P(CH_3)_3$[6] and $P(CF_3)_3$.[1] For molecules $P(CH_3)_nH_{3-n}$ and $P(CF_3)_nH_{3-n}$ with n = 1 and 2, the P-H bond length of 1.378 Å[5] was adopted while the valence angles around phosphorus were taken from those of $P(CH_3)_3$ and $P(CF_3)_3$, respectively. Results of our calculations are summarized in Table I, which reveals the following trends that are independent of n: (a) the P-C bond length of $P(CF_3)_nH_{3-n}$ is longer than that of $P(CH_3)_nH_{3-n}$, regardless of whether d orbitals are present on phosphorus or not; (b) either in $P(CH_3)_nH_{3-n}$ or in $P(CF_3)_nH_{3-n}$, the P-C bond length becomes shorter upon including d orbitals on phosphorus; (c) in each molecule the P-C overlap population is not decreased but enhanced by phosphorus d orbitals.

Thus our study shows that the role of phosphorus d orbitals in $P(CH_3)_3$ and $P(CF_3)_3$ is not counterintuitive but normal, in agreement with the observation of Collins et al.[5] In accounting for the long P-C bond of $P(CF_3)_3$, the concept of counterintuitive orbital interaction remains valid since it provides a mechanism by which electron density shifts from the electropositive region of P-C bond to the electronegative region of C-F bond.[4] However, this electron shift is not due to phosphorus d orbitals as indicated by the extended Hückel calculations.[1] Use of the weighted H_{ij} formula is found to greatly reduce the extent of counterintuitive orbital interaction in extended Hückel calculations on $P(CF_3)_3$, as in the case of molecules containing transition-metal atoms.[2]

Acknowledgment. This work was supported by the Research Corp. through a Cottrell Research Program, which is gratefully acknowledged. The authors are thankful to Professor I. G. Csizmadia and Drs. M. R. Peterson and R. A. Poirier for a copy of the MONSTERGAUSS program developed in their group. M.-H.W. is a Camille and Henry Dreyfus Teacher-Scholar, 1980-1985.

Registry No. $P(CH_3)_3$, 594-09-2; $P(CH_3)_2H$, 676-59-5; $P(CH_3)H_2$, 593-54-4; $P(CF_3)_3$, 432-04-2; $P(CF_3)_2H$, 460-96-8; $P(CF_3)H_2$, 420-52-0.

(6) L. S. Bartell and L. O. Brockway, *J. Chem. Phys.*, **32**, 512 (1960).
(7) Our calculations were carried out by employing the MONSTERGAUSS program written by M. R. Peterson and R. A. Poirier, Department of Chemistry, University of Toronto, Toronto, Canada.

Contribution from the Department of Chemistry, North Carolina State University, Raleigh, North Carolina 27650

Importance of the Out-of-Plane Niobium Displacement for the Semiconducting Property of $NbOX_2$ Net

M.-H. WHANGBO

Received September 23, 1981

Tight-binding band calculations were performed on $NbOCl_2$ net to examine the effect of Nb-Nb···Nb and Nb-O···Nb alternations on the electronic structure of $NbOCl_2$ net. The out-of-plane Nb displacement is found as crucial as the pairing distortion of Nb atoms for the semiconducting property of $NbOX_2$ net.

The crystal structure of two-dimensional $NbOX_2$ net[1-3] can be conveniently described in terms of a hypothetical $NbOX_4$ square pyramid **1**, in which the Nb atom is located at the

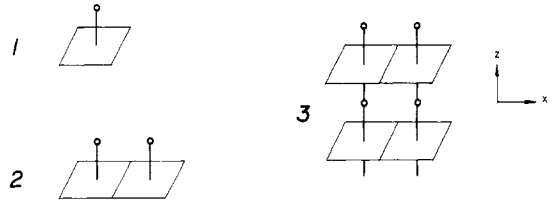

center of the X_4 plane. A one-dimensional $NbOX_2$ chain **2** is obtained when $NbOX_4$ pyramids are linked together by sharing their opposite edges. A two-dimensional $NbOX_2$ net **3** is derived when $NbOX_2$ chains are joined together by sharing their oxygen atoms. The real structure of $NbOX_2$ net differs from the ideal structure **3** in two important aspects: (a) there occurs a pairing distortion of Nb atoms in each $NbOX_2$ chain of **3**, leading to an alternation of two unequal Nb-Nb distances along the x axis (i.e., Nb-Nb···Nb alternation); (b) each Nb atom of **3** is displaced from the center of X_4 plane as depicted in **4a**, giving rise to an alternation of two unequal Nb-O bonds along the z axis (i.e., Nb-O···Nb alternation).[3]

Each $NbOX_2$ chain of **3** consists of Nb^{4+} (d^1) ions, so the occurrence of Nb-Nb···Nb alternation is an expected result just as in the case of NbX_4 chains.[4-7] Thus the semicon-

(1) H. G. Schnering and H. Wöhrle, *Angew. Chem.*, **75**, 684 (1963).
(2) H. Schäfer and H. G. Schnering, *Angew. Chem.*, **76**, 833 (1964).
(3) J. Rijnsdorp and F. Jellinek, *J. Less-Common Met.*, **61**, 79 (1978).
(4) D. R. Taylor, J. C. Calabrese, and E. M. Larsen, *Inorg. Chem.*, **16**, 721 (1977).
(5) D. G. Blight and D. L. Kerpert, *Phys. Rev. Lett.*, **27**, 504 (1971).
(6) M.-H. Whangbo and M. J. Foshee, *Inorg. Chem.*, **20**, 113 (1981).
(7) For the pairing distortion in low-dimensional materials, see: (a) J. S. Miller and A. J. Epstein, *Prog. Inorg. Chem.*, **20**, 1 (1976); (b) G. D. Stucky, A. J. Schultz, and J. M. Williams, *Annu. Rev. Mater. Sci.*, **7**, 301 (1977); (c) M.-H. Whangbo, *J. Chem. Phys.*, **75**, 4983 (1981).

0020-1669/82/1321-1721$01.25/0

Table I. Atomic Parameters[a,b]

χ_μ	ζ_μ	ζ_μ'	$H_{\mu\mu}$, eV
Nb 5s	1.90[6]		−10.1
Nb 5p	1.85		−6.86
Nb 4d	4.08 (0.6401)	1.64 (0.5516)	−12.1
O 2s	2.275		−32.3
O 2p	2.275		−14.8
Cl 3s	2.356[6]		−24.2
Cl 3p	2.039		−15.0

[a] The d orbitals are given as a linear combination of two Slater-type orbitals, and each is followed in parentheses by the weighting coefficient. [b] A modified Wolfsberg-Helmholz formula was used to calculate $H_{\mu\nu}$.[11]

ducting property of $NbOX_2$ net[3] may be attributed to the Nb–Nb···Nb alternation. However, it is not apparent whether or not the out-of-plane Nb displacement **4a** plays any sig-

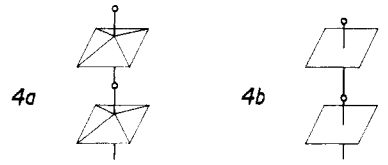

nificant role in determining the electronic properties of $NbOX_2$ net.[3] To explore this question, we have carried out tight-binding band calculations[6,8] on $NbOCl_2$ net based upon the extended Hückel method.[9] In the present work, the Nb–O, Nb–Cl, and Nb–Nb distances of the ideal $NbOX_2$ net **3** were respectively taken to be 1.97, 2.46, and 3.35 Å, which are the appropriate average values obtained from the crystal structure of $NbOCl_2$ net (e.g., Nb–O = 1.82, 2.11; Nb–Cl = 2.41, 2.51; Nb–Nb = 3.14, 3.56 Å).[2] And the Nb–Nb···Nb and Nb–O···Nb alternations were introduced into the ideal structure **3** in terms of the Nb atom displacements defined in **5a** and

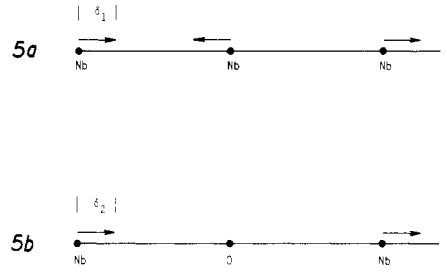

5b, respectively. The atomic parameters of Nb (4d, 5s, 5p), O (2s, 2p) and Cl (3s, 3p) orbitals employed in our calculations are summarized in Table I.

Figure 1 shows a portion of the d-block bands of the $NbOCl_2$ net with $\delta_1 = 0.2$ and $\delta_2 = 0.0$ Å. A unit cell of this net is $(NbOCl_2)_2$ so that, with all the bands lying below the $d_{x^2-y^2}{}^+$ band completely filled, two electrons are left to occupy the d-block bands of Figure 1. In Figure 1 the symbols $(x^2-y^2)^+$ and yz^- refer to the $d_{x^2-y^2}{}^+$ and $d_{yz}{}^-$ bands, respectively, and the meanings of these band labels are the same as those used in describing the band structure of NbX_4 chain.[6] The $d_{x^2-y^2}{}^+$ and $d_{yz}{}^-$ bands are largely made up of the unit cell orbitals shown in **6a** and **6b**, respectively. In contrast to the case of

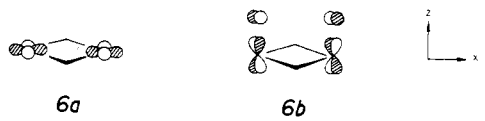

the $NbCl_4$ chain,[6] the $d_{x^2-y^2}{}^+$ and $d_{yz}{}^-$ bands of the $NbOCl_2$

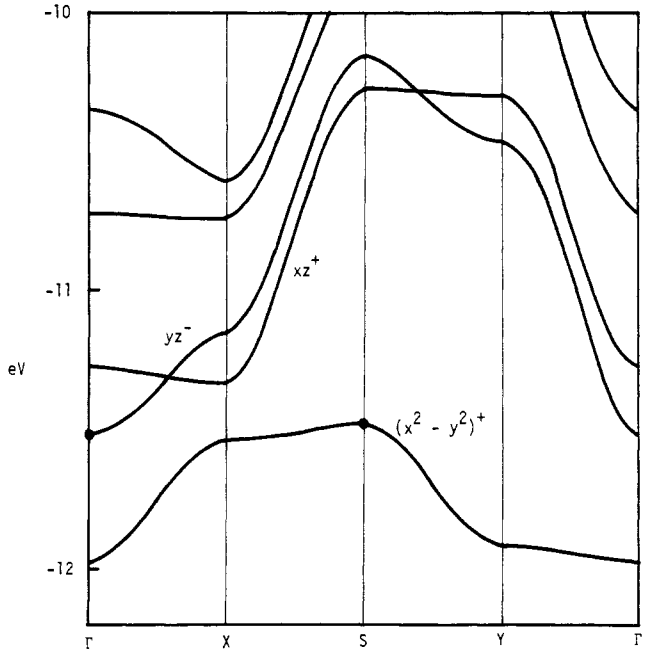

Figure 1. d-Block bands of $NbOCl_2$ net calculated for the case when $\delta_1 = 0.2$ and $\delta_2 = 0.0$ Å. The symbols Γ, X, S, and Y represent the reduced wave vectors (0, 0), (0.5, 0), (0.5, 0.5) and (0, 0.5), respectively. The Nb–Nb···Nb and Nb–O···Nb directions correspond respectively to the Γ → X and Γ → Y directions in the reciprocal space. The $d_{x^2-y^2}{}^+$ band top and the $d_{yz}{}^-$ band bottom were indicated by filled circles.

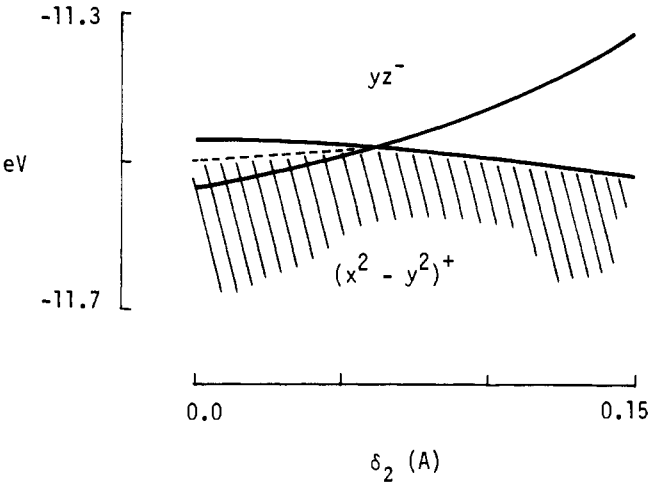

Figure 2. $d_{x^2-y^2}{}^+$ band top and the $d_{yz}{}^-$ band bottom plotted as a function of δ_2 for the case when $\delta_1 = 0.2$ Å. The shaded area indicates that each band orbital in this region is doubly occupied. The dashed line refers to the Fermi level.

net still overlap when the value of δ_1 is as large as 0.2 Å. Thus Figure 1 predicts a semimetallic property for $NbOCl_2$ net, in disagreement with experiment.[10] Consequently, the Nb–Nb···Nb alternation alone is not sufficient enough to reproduce the semiconducting property of $NbOCl_2$ net.[10]

The $d_{x^2-y^2}{}^+$ band top occurs at S, while the $d_{yz}{}^-$ band bottom occurs at Γ. In our calculations, the relative position of these two energy points is found to determine the presence or absence of a band gap. In the $d_{x^2-y^2}{}^+$ band the $d_{x^2-y^2}$ orbital of each Nb atom combines out-of-phase with bridging halogen orbitals. Thus the extent of this antibonding interaction is reduced by

(8) M.-H. Whangbo and R. Hoffmann, *J. Am. Chem. Soc.*, **100**, 6093 (1978).
(9) R. Hoffmann, *J. Chem. Phys.* **39**, 1397 (1963).
(10) D. L. Kerpert and R. E. Marshall, *J. Less-Common Met.*, **34**, 153 (1974).
(11) J. H. Ammeter, H.-B. Bürgi, J. C. Thibeault, and R. Hoffmann, *J. Am. Chem. Soc.*, **100**, 3686 (1978).

the out-of-plane displacement **4a** as depicted in **7a**. The d_{yz}^-

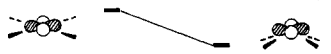

7a

7b

band at Γ has the nodal property shown in **8** along the *z* axis,

8

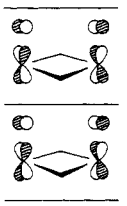

in which the interaction between Nb and O is antibonding within a chain but bonding between neighboring chains. Thus the out-of-plane Nb displacement **4a** would enhance the antibonding but decrease the bonding interaction. Figure 2 shows how the $d_{x^2-y^2}^+$ band top and the d_{yz}^- band bottom vary as a function of δ_2 when $\delta_1 = 0.2$ Å. As expected from the above discussion, the out-of-plane Nb displacement **4a** is found to slightly lower the $d_{x^2-y^2}^+$ band but greatly raise the d_{yz}^- band, eventually giving rise to a band gap beyond a certain value of δ_2. The repeat unit of the $NbOX_2$ net with $\delta_1 = 0$ and $\delta_2 \neq 0$ is $(NbOX_2)$, and thus there exists one electron per unit cell to fill the d-block bands. Such an $NbOX_2$ net cannot become semiconducting as in the case of NbX_4 chain with no Nb–Nb···Nb alternation.[6] Therefore, the out-of-plane Nb displacement is as crucial as the pairing distortion of Nb atoms for the semiconducting property of $NbOX_2$ net.

An alternative way of introducing Nb–O···Nb alternation into **3** is shown in **4b**, which shows a displacement of the oxygen atoms in each $NbOX_2$ chain of **3** toward the Nb atoms that are held in the X_4 planes. It is not **4b** but **4a** that is observed. The preference of **4a** over **4b** may be due in part to the stabilization of the $d_{x^2-y^2}^+$ band, which arises from the distortion **4a** as indicated in **7a**. When the Nb–O···Nb alternation is introduced as in **4b** into the $NbOX_2$ net with $\delta_1 = 0.2$ Å, our calculations show the $d_{x^2-y^2}^+$ and d_{yz}^- bands to remain overlapping for the oxygen atom displacement of as large as 0.2 Å. Incidently, the distortion **4a** leads to a rehybridization of the d_{yz} orbital as shown in **7b**. As a consequence of the energy level changes indicated in **7a** and **7b**, the distortion **4a** becomes more efficient than the alternative **4b** in introducing a band gap into $NbOX_2$ net.

Acknowledgment. This work was supported by the donors of the Petroleum Research Fund, administered by the American Chemical Society. The author wishes to thank Professor T. M. Rice for his valuable comment on this work. M.-H.W. is a Camille and Henry Dreyfus Teacher-Scholar, 1980–1985.

Registry No. $NbOCl_2$, 13867-44-2.

Contribution from the Francis Bitter National Magnet Laboratory, Massachusetts Institute of Technology, Cambridge, Massachusetts 02139, the Department of Chemistry, Harvard University, Cambridge, Massachusetts 02138, and Bell Laboratories, Murray Hill, New Jersey 07974

Antiferromagnetic Exchange Interactions in $[Fe_4S_4(SR)_4]^{2-,3-}$ Clusters

G. C. PAPAEFTHYMIOU,*[1a] E. J. LASKOWSKI,[1b] S. FROTA-PESSÔA,[1a] R. B. FRANKEL,[1a] and R. H. HOLM[1c]

Received July 27, 1981

The exchange coupling of Fe atoms in the mixed-valence clusters $[Fe_4S_4(SPh)_4]^{2-}$ and $[Fe_4S_4(SPh)_4]^{3-}$, synthetic analogues of [4Fe–4S] sites in ferredoxin proteins, has been examined in terms of a theoretical treatment of previously reported magnetic susceptibility and magnetization properties. Both clusters exhibit antiferromagnetic behavior at 4.2–338 K. The isotropic exchange Hamiltonian

$$\mathcal{H} = g\mu_B \sum_{i=1}^{4} \vec{H}\cdot\vec{S}_i - 2\sum_{i<j} J_{ij}\vec{S}_i\cdot\vec{S}_j$$

is used to parameterize the results in terms of the exchange constants J_{ij}. It is shown that a single value of J_{ij} does not produce satisfactory results for either cluster oxidation level. Allowing J_{ij} to have different values for coupled Fe sites in different combinations of Fe(II,III) oxidation states affords an accurate simulation of the temperature dependence of the magnetic susceptibility of $(Et_4N)_2[Fe_4S_4(SPh)_4]$. The best simulation was obtained with $J_{ij}(Fe^{3+} \rightleftarrows Fe^{3+}) = -275$ cm^{-1}, $J_{ij}(Fe^{2+} \rightleftarrows Fe^{2+}) = -225$ cm^{-1}, and $J_{ij}(Fe^{3+} \rightleftarrows Fe^{2+}) = -250$ cm^{-1}. For $(Et_4N)_3[Fe_4S_4(SPh)_4]$ a reasonable simulation of both the susceptibility and the magnetization results (at 4.2 K) was obtained with two independent J_{ij} values, $J_{ij}(Fe^{3+} \rightleftarrows Fe^{2+}) \approx -60$ cm^{-1} and $J_{ij}(Fe^{2+} \rightleftarrows Fe^{2+}) \approx -40$ cm^{-1}. The addition of a single electron to the [4Fe–4S] core unit is seen to produce a large decrease in the magnitude of the exchange constants. A similar behavior has been observed in the susceptibility properties of oxidized and reduced 2-Fe protein sites $[Fe_2S_2(Cys\text{-}S)_4]$. Limitations of the theoretical treatment are discussed.

Introduction

The synthesis and detailed structural and physicochemical characterization of the cubane-type clusters $[Fe_4S_4(SR)_4]^{2-,3-}$ have been previously reported.[2-11] These results have demonstrated the isoelectronic nature of the synthetic species with certain oxidation levels of the $[Fe_4S_4(Cys\text{-}S)_4]$ electron-transfer

(1) (a) Massachusetts Institute of Technology. (b) Bell Laboratories. (c) Harvard University.

(2) J. Cambray, R. W. Lane, A. G. Wedd, R. W. Johnson, and R. H. Holm, *Inorg. Chem.*, **16**, 2565 (1977).

(3) R. W. Lane, A. G. Wedd, W. O. Gillum, E. J. Laskowski, R. H. Holm, R. B. Frankel, and G. C. Papaefthymiou, *J. Am. Chem. Soc.*, **99**, 2350 (1977).

0020-1669/82/1321-1723$01.25/0